05,10

Coexistence of ferromagnetism and superconductivity in orthorhombic phase microparticles of the topological superconductor Mo_2C

© M.V. Bakhmetiev[1,2], E.V. Dvoretskaya[1], S.N. Kashin[1,2], V.V. Savin[2], R.B. Morgunov[1,2,3,¶]

[1] Federal Research Center of Problems of Chemical Physics and Medicinal Chemistry RAS, Chernogolovka, Russia
[2] Immanuel Kant Baltic Federal University, Kaliningrad, Russia
[3] Tambov State Technical University, Tambov, Russia

¶ E-mail: bakhmetiev.maxim@gmail.com

Received December 4, 2025
Revised February 12, 2026
Accepted February 12, 2026

The coexistence of ferromagnetism and superconductivity in β-Mo_2C microparticles produced by pyrolysis was discovered. The dependences of the critical temperature (T_C) and critical magnetic field (HC) of the superconducting state on the particle size of molybdenum carbide were obtained. As the microparticle diameter increases from 0.2 μm to 5 μm, the critical temperature of superconductivity decreases from 7.2 K to 3.7 K, and at a diameter of 10 μm, superconductivity is not detected in the studied temperature range from 2 K. The coercivity of the sample also decreases with increasing particle size, however, the samples remain ferromagnetic and retain a non-zero coercivity up to 300 K. The presence of ferromagnetism is explained by defects in the crystalline structure of the microparticles.

Keywords: molybdenum carbide, microparticles, type II superconductivity, critical temperature, critical field.

DOI: 10.61011/PSS.2026.02.63383.8855

1. Introduction

Superconductivity in small particles and coexistence of „antagonistic“ ferromagnetism and superconductivity are relevant issues, since if these phenomena are explained it will provide an insight into the fundamental limitations of the superconducting state, and also give the information about transition from bulk materials to the reduced dimension systems [1,2]. One of the key issues is the existence of a minimum characteristic size when superconductivity can still be maintained, as well as the effect of the energy spectrum discreteness, surface states, and microstructural inhomogeneity on the critical parameters of the superconducting state.

The fundamental limit of the minimum size of a superconducting particle is determined by Anderson criterion [1,2]: superconductivity disappears when the distance between single-electron levels is comparable to the energy slit [3]. For metals, this corresponds to particle sizes of several nanometers, but interparticle interaction, defects and surface can significantly change the behavior of the system [4,5]. Experiments show that in ultra-small particles (e.g., Ga $\sim$ 1.4 nm) the superconductivity is possible due to weak charge transfer between particles, despite a formal violation of the Anderson criterion [6,7]. In granular systems, the Josephson coupling between polycrystal grains plays a crucial role, determining transition between the phase-coherent superconducting and insulating states [8].

Another superconducting material that is currently of interest is molybdenum carbide [1,9,10]. Molybdenum carbide in various phases behaves as type-II superconductor [1]. The size and structure of microparticles Mo_2C depend on pyrolysis conditions The particles with a size of < 5 nm form in the phase α-Mo_2C, and larger particles with a diameter > 50 nm form in β-Mo_2C phase at a temperature of 850 °C [1,10]. These two phases exhibit superconductivity with a critical temperature of T_C in the range 6.7−7.3 K and 8.1−12.2 K respectively. The possibility of obtaining Mo_2C microparticles of these phases from a matrix system based on carboranylene siloxane obtained from Mo makes them an ideal system for studying dimensional effects affecting the corresponding superconducting properties of the two phases. In addition, ultrathin films of transition metal carbides represent a class of developing two-dimensional (2D) materials with superconductivity and demonstrate great potential for electric power storage and other applications. Low-temperature magnetotransport of ultrathin 2D superconducting crystals α-Mo_2C synthesized by chemical deposition from the gas phase was studied in [9]. The magnetoresistance curves show reproducible oscillations in weak magnetic fields at temperatures significantly lower than the temperature of the superconducting transition of

crystals. In [9] it is shown that the oscillatory behavior of magnetoresistance is a consequence of shielding currents circulating around the boundary of triangular terraces found on the surface of ultrathin crystals Mo_2C. As the thickness Mo_2C decreases, the crystals exhibit negative magnetoresistance in the superconducting transition mode, which reveals strong phase fluctuations in superconducting parameters associated with the superconductor-insulator transition. These results show that superconducting nanocrystals Mo_2C represent a two-dimensional crystalline superconductor system with increased quantum fluctuations. Phase β-Mo_2C demonstrates a superconducting state with a full slit, while its electronic band structure assumes the presence of doubly degenerate nodal surfaces and fourfold degenerate nodal lines. The phonon dispersion spectrum Mo_2C provides the lowest total energy in case of the orthorhombic β-phase (with the space group P_{bcn}), which is consistent with experiment. The magnetization measurements confirm the bulk superconductivity of β-Mo_2C with a critical transition temperature of $T_C = 3.2$ K.

The dependence of critical temperature of superconductors T_C on the diameter of particles d or films thickness is described in many studies [11–13]. With the growth of diameter of Pb particles the critical temperature T_C rises, and for Al, visa versa, T_C declines [11,12]. The increasing dependence $T_C(d)$ is explained by Kubo model for the particles [11], which takes into account the splitting of energy sublevels in the conduction band or valence band of the particle. The decreasing dependence $T_C(d)$ is explained by a change in the strength of the electron-phonon bond in the surface region of superconducting bodies [11–13]. This model is in good agreement with experimental data for several type-II superconductors [11–13], which include molybdenum carbide considered in this paper.

Although the ideal crystal lattice of β-Mo_2C is diamagnetic, vacancies and impurity atoms have uncompensated magnetic moments, and with a large number of them characteristic of microparticles, as well as with a significant contribution from the surface of microparticles, they can be bound by exchange interaction and exhibit ferromagnetism.

The purpose of our work is to study the dependences of the critical temperature and the critical field of microparticles of the type-II superconductor Mo_2C on their diameter while simultaneously controlling the magnetism created by the spins of defective states of molybdenum carbide or impurity.

2. Methodology and samples

The industrial particles of molybdenum carbide with an average diameter $d \sim 0.2\,\mu$m, $0.4\,\mu$m, $0.8\,\mu$m, $2\,\mu$m, $5\,\mu$m, $10\,\mu$m (Rusgraphene) were examined in the study. Particles with an average diameter of $d \sim 0.2-0.8\,\mu$m were obtained by pyrolysis at a temperature of 1000°C, and particles with $d \sim 2-10\,\mu$m at a temperature of $T = 1250\,^\circ$C. Pyrolytic transformations of crosslinked mesh matrices formed from inorganic-organic hybrid carbonanylene siloxane oligomers obtained from Mo result in formation of ceramic mixtures containing Mo_2C microparticles of controlled sizes. Samples with different average particle sizes were obtained by mechanical grinding. No additional chemical reagents were used in the post-treatment process.

Table 1. Mass fraction of transition metals in Mo_2C powders with different microparticle diameters, obtained by XRF method

Diameter of microparticles Mo_2C	Concentration, mass %		
	Fe	Co	Mo
$10\,\mu$m	0.25622	0.13859	99.60479
$5\,\mu$m	0.25284	0.25033	99.49683
$2\,\mu$m	0.35248	0.11280	99.53472
$0.8\,\mu$m	0.26219	0.13957	99.59824
$0.4\,\mu$m	0.22514	0.21165	99.56321
$0.2\,\mu$m	0.24147	0.18352	99.57501

Figure 1 shows the X-ray fluorescence (XRF) spectra of Mo_2C $0.8\,\mu$m powder obtained using various crystal analyzers in a wide range of wavelengths. Table 1 shows the integral percentage concentration of transition metals Fe, Co contained in Mo_2C powders with different microparticle diameters obtained by XRF method.

The total average value of ferromagnetic impurities of Fe and Co in Mo_2C powders is 0.44 mass.%, while in all powders an average of 1.74 times more Fe than Co is observed. The proportion of Fe and Co impurities does not change in powders with different average particle diameters.

X-ray diffraction analysis (XRDA) was performed on PANalytical Aeris X-ray diffractometer. The images were taken in the Bragg-Brentano geometry in 2θ angles range from 20 to 80 degrees in increments of 0.012 degrees. The phases obtained on the diffraction spectrum were identified using PDF4+ crystallographic database. The X-ray diffraction spectrum for Mo_2C with a particle diameter of $0.8\,\mu$m (Figure 2) contained reflexes corresponding to Mo_2C, which is confirmed by coincidence of experimentally studied reflexes with peaks from the powder database PDF No. 000-72-1683 for a rhombic crystal lattice. The X-ray diffraction spectrum matches with the spectrum obtained in [1] for β-phase of Mo_2C.

The particle images (Figure 3) were obtained using Zeiss Supra 25 scanning electron microscope (SEM).

The particle size distribution was obtained by laser diffraction using a laser particle size analyzer LASKA-TD (sizes of the analyzed particles $0.1-1000\,\mu$m) (Figure 4, Table 2). The laser diffraction method is implemented as follows: a laser beam passes through a container with a suspension of particles in distilled water, causing light scattering at various angles, while the intensity of the

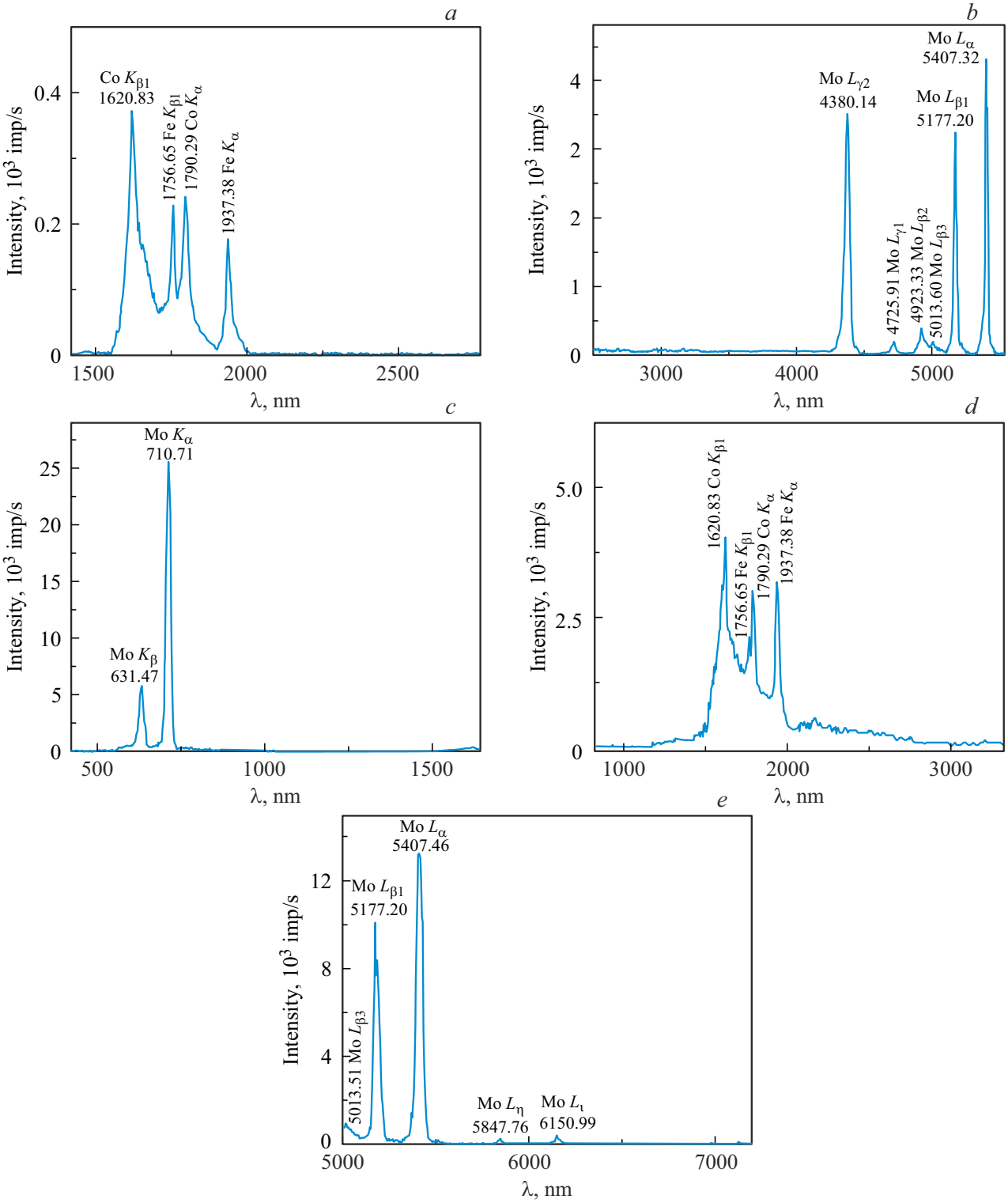

Figure 1. XRF spectra of Mo_2C 0.8 μm powder produced in various crystal-analyzers: *a* — C(002)1, *b* — C(002)2, *c* — LiF(200)1, *d* — LiF(200)2, *e* — Pentaerythritol (PET).

scattered radiation is recorded by a special multi-channel sensor. By the nature of the intensity change relative to the scattering angles, the particle size is determined and the particle size distribution is plotted. LaSca32 algorithm was used to evaluate the particle size distribution function. The quantitative granulometric (fractional) composition was characterized by distribution quantiles (D10, D25, D50, D75, D99), representing the proportion of particles with

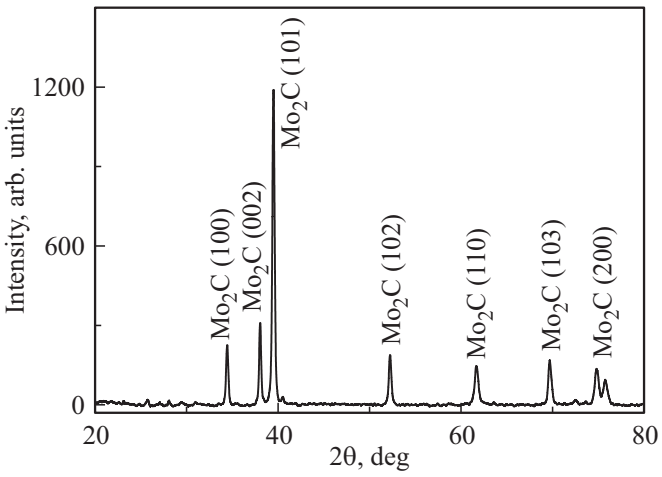

Figure 2. X-ray diffraction spectrum of β-Mo_2C.

sizes smaller than this one. Table 2 shows the fractional distribution of diameters d of Mo_2C particles by quantiles. Every next size class includes the previous one, AVG (average) — the arithmetic mean at each measurement point. Thus, the value of quantile D50 = 10.13 suggests that in the studied sample 50 % of particles had a diameter of 10.13 μm and less, D75 = 12.98−75 % of particles had a diameter of 12.98 μm and less.

The dependences of the magnetic moment on magnetic field and on temperature were measured using an MPMS 5XL Quantum Design SQUID magnetometer.

3. Experimental results

Figure 5 shows the temperature dependences of magnetization of the studied powders obtained after cooling the particles in a zero magnetic field (ZFC) with subsequent heating in 50 Oe field. It can be seen that the temperature of transition to the superconducting state depends on the size of molybdenum carbide particle.

Magnetic hysteresis loops were obtained, which are shown in Figure 6. For non-superconducting samples with a particle size of 10 μm, magnetic hysteresis is observed, typical for a ferromagnetic material, while for superconducting samples with a particle size of $\leq 5\,\mu$m, a curve with a maximum and minimum is observed along with a conventional ferromagnetic hysteresis loop near zero field.

Such curves are typical for a superconductor co-existing with ferromagnetism. It can be seen that for the particles with a diameter of 10 μm no superconductivity is observed at 2 K. The critical size at which superconductivity is achieved at the lowest temperature available to us, 2 K, is 5 μm.

Next, we obtained the temperature dependences of magnetization in the temperature range of superconductivity from 2 to 7.4 K with a step of 0.2 K in the field from 0 Oe to the critical field H_C for each sample, from which we then plotted the magnetization diagrams. Figure 7 illustrates the magnetization diagrams of Mo_2C with a different most probable diameter of 0.2−5 μm. From these dependencies, critical temperatures T_C and critical fields H_C were determined, shown in Figure 8, *a*, 8, *b* and 8, *c*, as functions of diameter and temperature, respectively.

Since the magnetization curves contain contributions from a superconductor and a ferromagnet, we determined the coercive force of the ferromagnet H_F from the most probable particle diameter (Figure 8, *d*) and from temperature (Figure 8, *e*). From Figure 8, *d* and 8, *e* we may see that the growth of the particle diameter leads to the reduced coercive force H_F. However, a nonzero coercive force is observed up to 300 K, indicating a very high Curie temperature in the studied microparticles.

4. Discussion

With the decrease in the particles average size the transition temperature T_C from 3.2 K at $d = 5\,\mu$m to 4.8 K at $d = 0.4\,\mu$m can be observed. For the smallest particles studied in our work with $d = 0.2\,\mu$m, the critical temperature id equal $T_C \approx 7.2 \pm 1$ K. Thus, for microparticles Mo_2C, a monotonously decreasing dependence T_C (d) is observed with the growing particle size (Figure 8, *a*).

This behavior is qualitatively consistent with previously observed dimensional effects in the type-II superconductors, for which a decrease in particle size leads to an increase in the influence of surface states and defects [11,12]. In such systems, changes in conditions of electron-phonon interaction near the surface and on defects can lead to an increase in the critical temperature compared to the bulk state. In case of Mo_2C microparticles, the dimensional effect is apparently not directly related to the geometry of the particle as a whole object, but reflects the presence of a spatially inhomogeneous, probably granular, superconducting structure. This is evidenced by wide superconducting transitions, a complex magnetic response, and the coexistence of superconductivity with ferromagnetism. This pattern may be due to the presence of nanoscale superconducting regions or domains inside the microparticles, which form an effective average value T_C, depending on the total particle size.

Figure 8, *b* shows the line representing the approximation of $H_C(T)$ by the formula [15]:

$$H_C(T) = H_C(0)\left[1 - \left(\frac{T}{T_C}\right)^2\right], \qquad (1)$$

where $H_C(0)$ — the value of the critical field at absolute zero temperature. The values of critical field at $T = 0$ grow with the increasing particle diameter. At 0.2 μm the value $H_C(0)$ reaches 1.15 T.

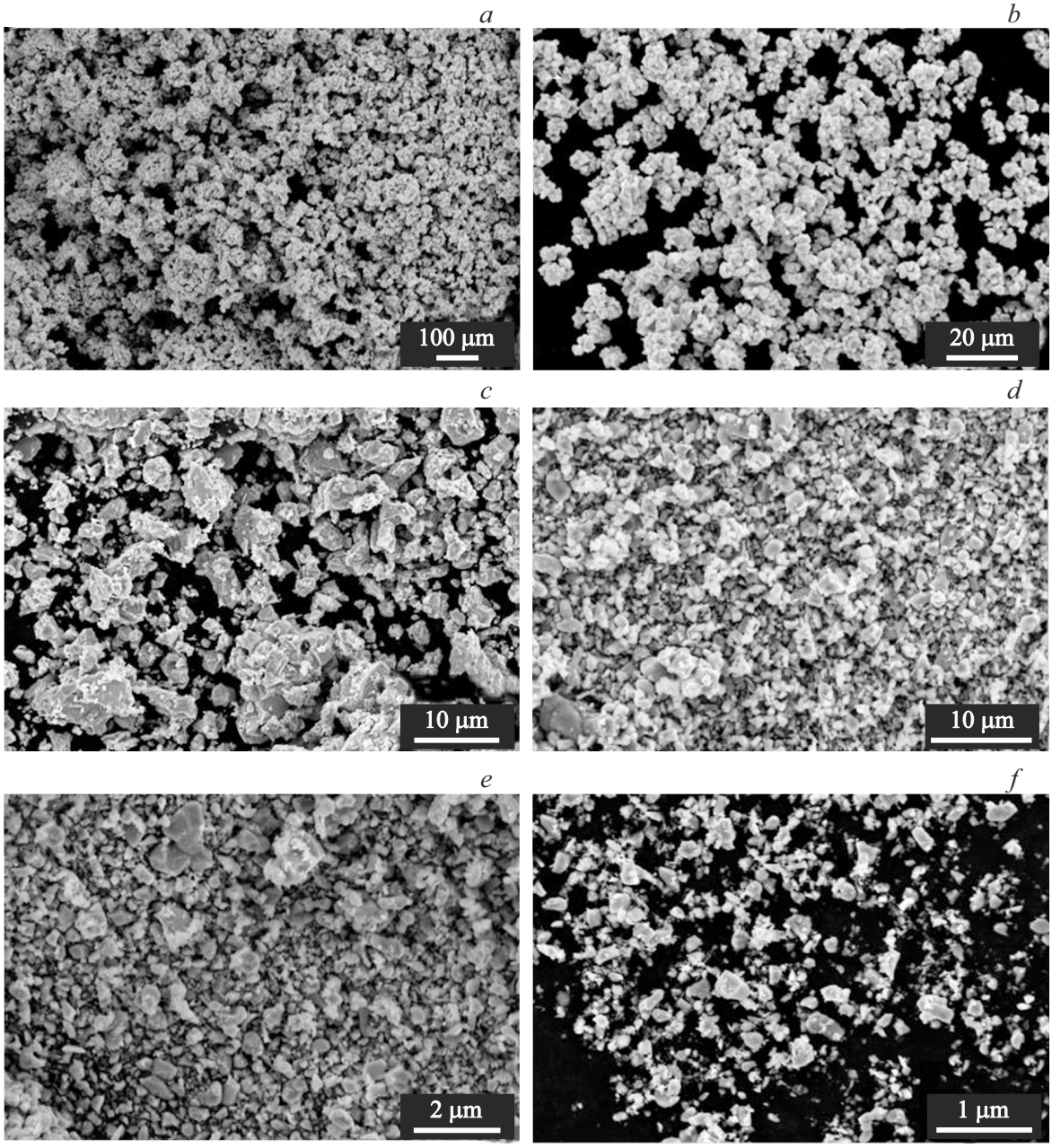

Figure 3. SEM images of Mo_2C particles with the most probable diameters $10\,\mu$m (*a*), $5\,\mu$m (*b*), $2\,\mu$m (*c*), $0.8\,\mu$m (*d*), $0.4\,\mu$m (*e*), $0.2\,\mu$m (*f*).

Let us now discuss the observed ferromagnetic hysteresis loop. The saturation magnetization of one formula unit at $T = 300\,\mathrm{K}$, expressed in Bohr magnetons, for one Mo atom is

$$\mu_{Mo_2C} = (204\,\mathrm{g/mol} \cdot 3.9 \cdot 10^{-3}\,\mathrm{emu})/$$
$$(27 \cdot 10^{-3}\,\mathrm{g} \cdot 927.4 \cdot 10^{-23}\,\mathrm{erg/Oe} \cdot 6 \cdot 10^{23}\,\mathrm{mol}^{-1})$$
$$= 5.3 \cdot 10^{-3}\,\mu\mathrm{B}.$$

This means that ferromagnetism involves 5 out of 1000 particles in the entire sample. This behavior is caused by impurities in Mo_2C powder, which was detected using XRF (Figure 1 and Table 1). This, for instance may include FeMo, Fe_3C or FeCo alloys. XRF measurements show that the iron concentration is the same for all powders within the experimental margin of error. However, the magnitude of the observed ferromagnetic signal is too large to be explained solely by this permanent Fe content. This suggests that, in addition to external iron impurities, there may be an additional magnetic contribution associated with Mo_2C particles. Moreover, the dependence of the sample's coercive force on the size of molybdenum

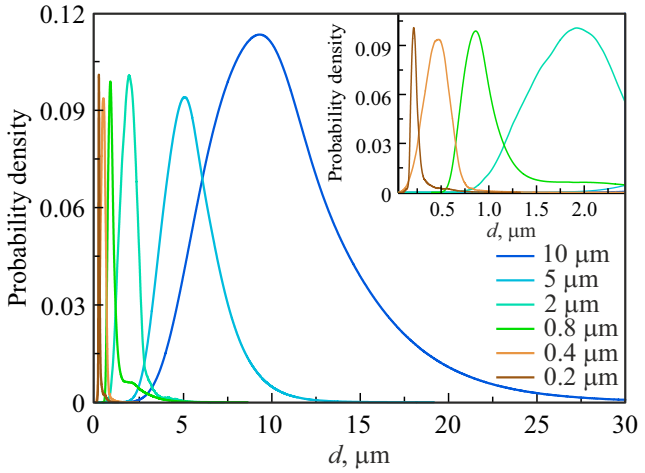

Figure 4. Probability distribution for diameters d of Mo_2C particles with maxima at 10 μm (a), 5 μm (b), 2 μm (c), 0.8 μm (d), 0.4 μm (e), 0.2 μm (f).

Table 2. Integral granulometric (fractional) composition in μm of Mo_2C particles— fractional particles distribution by quantiles. Every next size class includes the previous one. AVG — the arithmetic mean at each measurement point

Quantile	Mo_2C 10 μm	Mo_2C 5 μm	Mo_2C 2 μm	Mo_2C 0.8 μm	Mo_2C 0.4 μm	Mo_2C 0.2 μm
D10 =	6.19	3.76	1.31	0.56	0.28	0.18
D25 =	7.85	4.47	1.55	0.67	0.38	0.20
D50 =	10.13	5.39	1.82	0.81	0.46	0.23
D75 =	12.98	6.53	2.25	0.98	0.54	0.27
D90 =	16.53	7.80	2.81	1.17	0.72	0.54
D99 =	24.35	10.71	3.72	1.61	0.84	0.58
AVG	10.83	5.61	1.91	0.82	0.48	0.21

carbide microparticles directly indicates the presence of ferromagnetism in Mo_2C particles themselves.

Microparticles of molybdenum carbide (MoC_x) are usually diamagnetic, but some researchers have observed ferromagnetic properties in certain forms of microparticles, especially in combination with other elements or with a certain structure. Magnetic composites such as Ni/Mo_2C or Mo_2C/NC alloyed with cobalt may serve as an example. Ferromagnetism is caused by a specific nanostructure, defects, or doping that can disrupt the symmetry of the material and cause ferromagnetism that is absent in a perfect lattice. For example, it can be observed in the two-dimensional η-phase of molybdenum carbide.

It follows from our experiments that molybdenum carbide can exhibit both superconductivity and ferromagnetism, a phenomenon in which these two properties can coexist, but their relationship is complex and often requires a finely tuned balance. It follows from our experiments that molybdenum carbide can exhibit both superconductivity and ferromagnetism, a phenomenon in which these two properties can coexist, but their relationship is complex and often requires a finely tuned balance [16].

Ferromagnetism is usually incompatible with super conductivity, but there are several different types of superconductors in which these two phenomena are not only compatible, but are also interrelated. The coexistence of superconductivity and magnetism critically depends on how these two subsystems are related. The most important thing is which of the two subsystems is „the strongest“, i. e. which of the two critical temperatures is greater: Curie temperature of the magnetic ordering T_F or the critical temperature of superconductivity T_C. In such compounds as UGe_2, URhGe or UCoGe [17–19], as

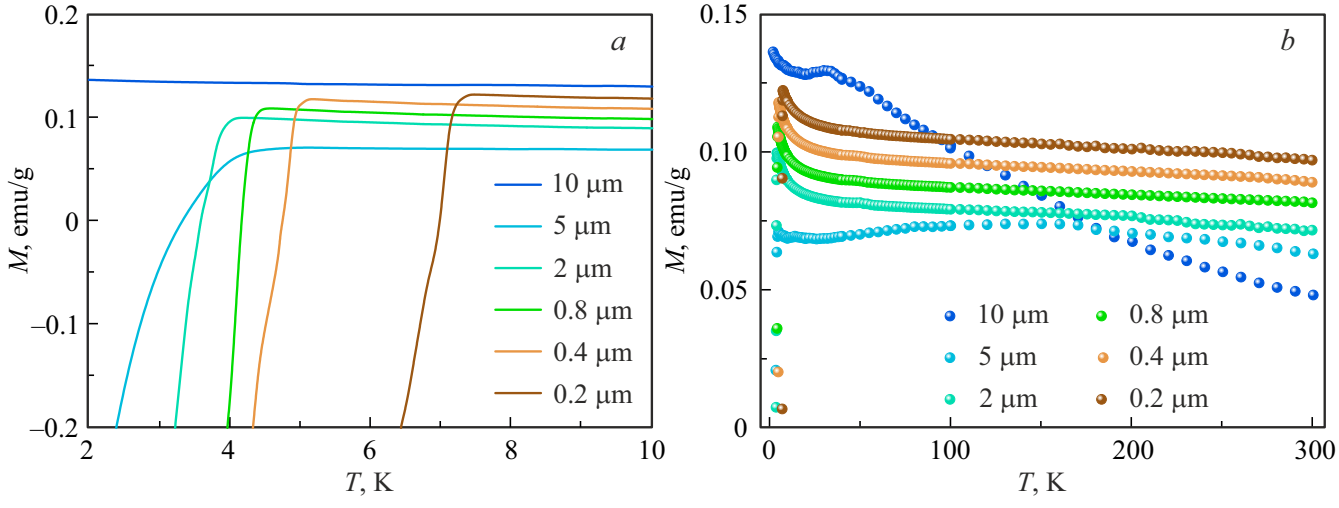

Figure 5. Temperature dependences of the magnetization of molybdenum carbide particles in the range from 2 to 10 K (a) and in the range from 2 to 300 K (b) obtained in ZFC conditions. The measuring field made 50 Oe.

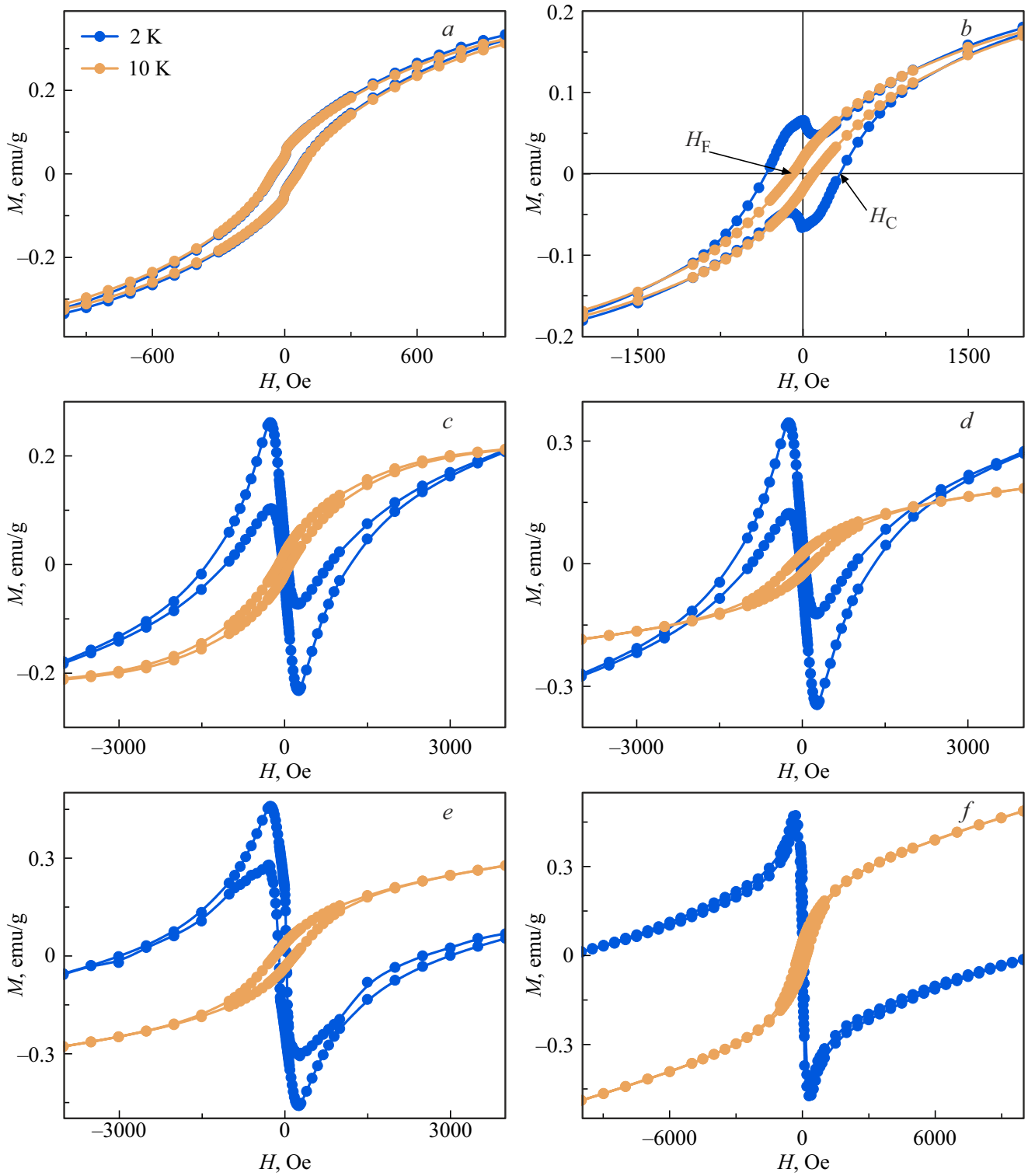

Figure 6. Magnetization hysteresis loops for Mo_2C particles with diameters 10 μm (*a*), 5 μm (*b*), 2 μm (*c*), 0.8 μm (*d*), 0.4 μm (*e*), 0.2 μm (*f*). The coercive force H_F and the critical field of the superconducting transition H_C are shown by arrows in Figure 6, *b*.

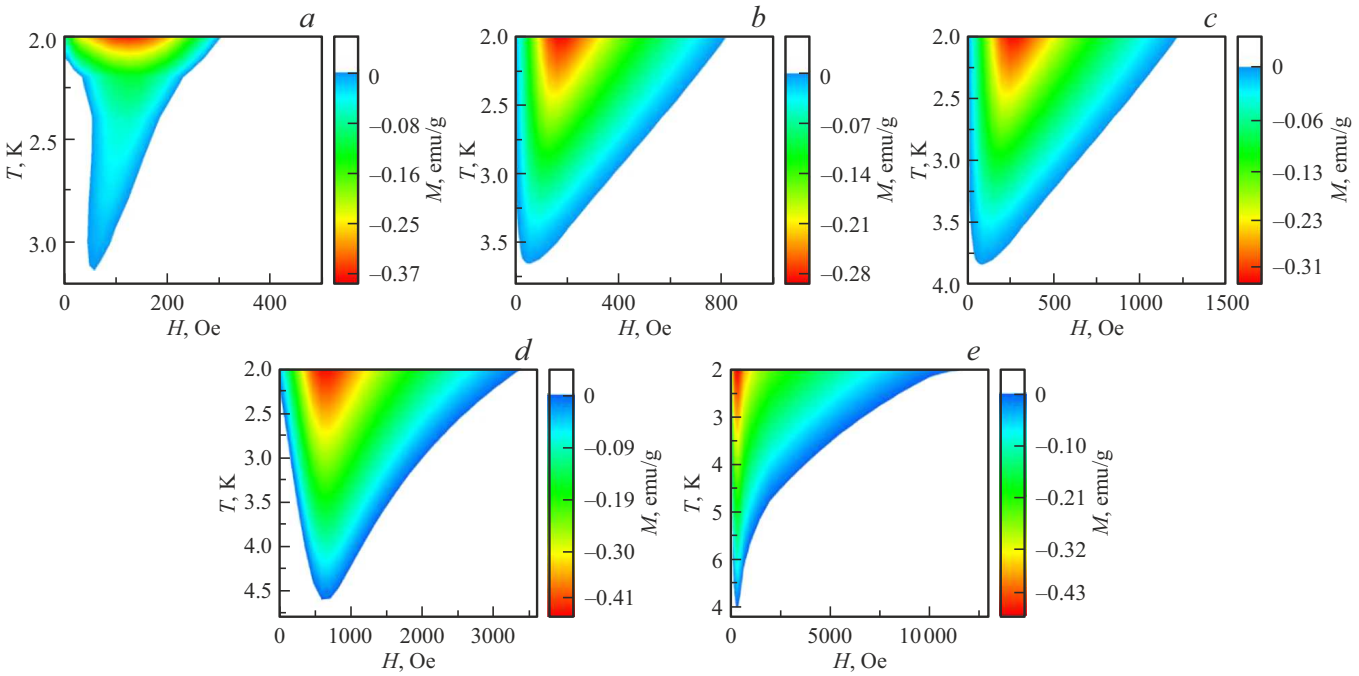

Figure 7. Magnetization diagrams of Mo_2C with a different most probable diameter: 5 μm (*a*), 2 μm (*b*), 0.8 μm (*c*), 0.4 μm (*d*), 0.2 μm (*e*).

well as $Ho_{1.2}Mo_6S_8$, $ErRh_4B_4$ and $ZrZn_2$ [20–22], the temperature of transition to superconductivity is lower than Curie temperature $T_C \ll T_F$. In such compounds, which include the studied microparticles, the interaction between the magnetic moments of atoms and free electron spins is controlled by the exchange mechanism. In this case, singlet electron pairing is suppressed, and superconductivity with triplet pairing occurs, which provides only minor corrections to the predominantly ferromagnetic state of [17–22].

In [23], the superconducting properties of β-phase of Mo_2C were reported, which were studied using measurements of magnetization and relaxation and rotation of the muon spin (μSR). No ferromagnetism of this phase, grown by the electric arc method, was detected in that work. The authors found that the temperature dependence of the superfluid density reveals a nodeless superconducting state, which is well described by the isotropic *s*-wave model. The absence of spontaneous magnetic fields below T_C indicates that time reversal symmetry is preserved in the superconducting state of Mo_2C in the absence of the field. Obviously, the presence of a ferromagnetic phase in our experiments should change the time reversal symmetry. The electronic band structure analysis shows that the density of states at Fermi level is determined by Mo-4*d*-electrons, while the contribution of C-2*p*-electrons is negligible over a wide range of energies. As a result, *p*-*d*-hybridization is rather weak in β-phase of Mo_2C, which leads to a relatively low value of T_C. β-Mo_2C carbide is a potential candidate for the study of topological superconductors combining ferromagnetic properties.

5. Conclusions

The existence of ferromagnetism with Curie temperature $T_F > 300$ K and superconductivity with a critical temperature $T_C = 3.7-7.2$ K for the particles in 0.2–8 μm range was discovered. In this paper, the dependence of the critical temperature (T_C) and the critical magnetic field (H_C) of the superconducting transition of Mo_2C molybdenum carbide particles on their most probable diameter is studied. The results obtained demonstrate that as the particle size shrinks, an increase in T_C is observed, which indicates the impact of nanoscale effects on parameters of the type-II superconductivity. The coercive force of the ferromagnetic state decreases sharply in the range 2–8 K, which practically coincides with the superconductivity domain, however, even at high temperatures up to 300 K, the sample remains ferromagnetic, exhibiting a nonzero coercive force. The dependence of sample's coercive force on the average particle size of molybdenum carbide at permanent mass fraction of the impurity in all samples indicates the presence of ferromagnetism in Mo_2C particles themselves.

Funding

The study was carried out within the grant of the Russian Science Foundation No. 25-72-31032, https://rscf.ru/project/25-72-31032/.

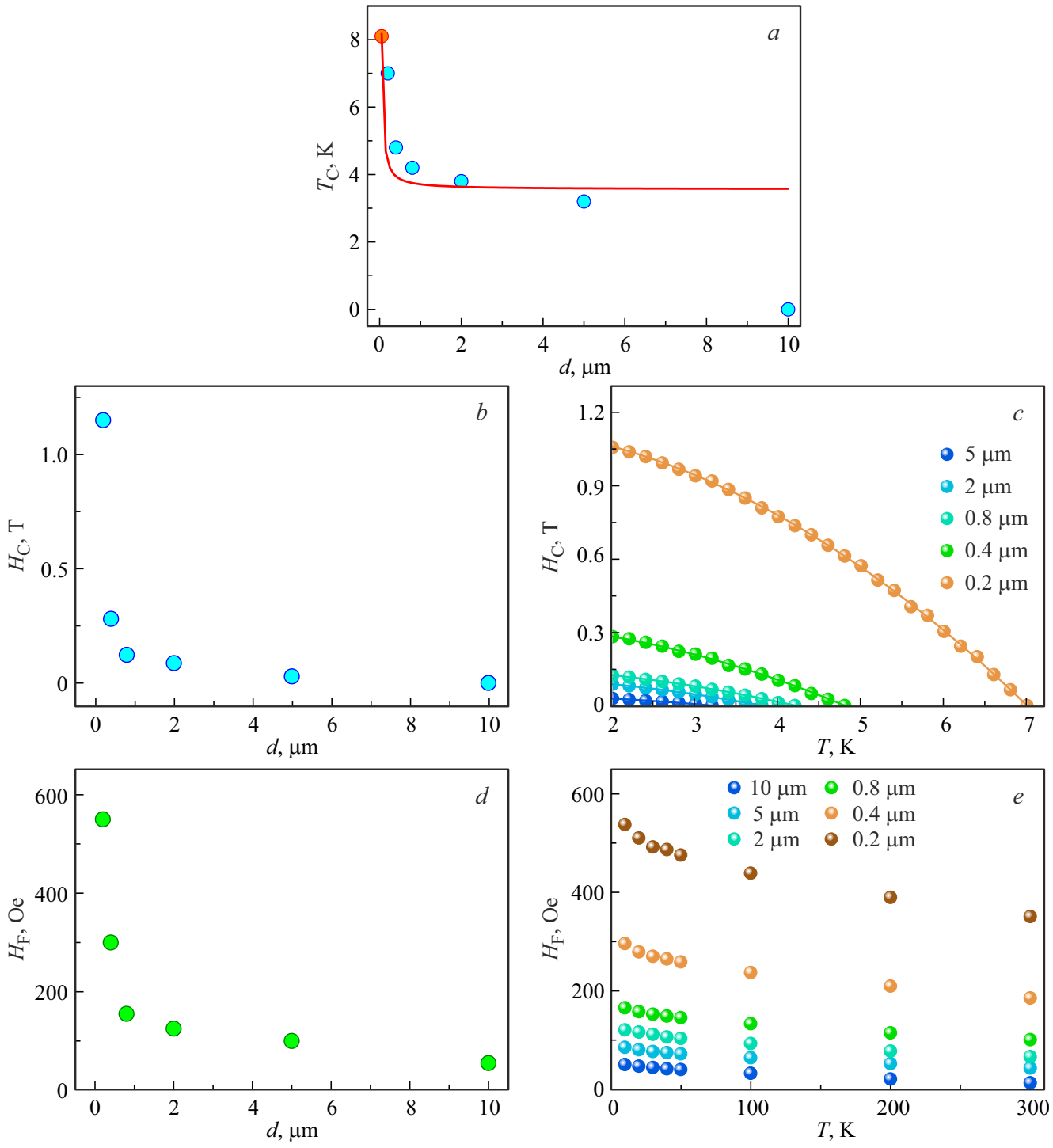

Figure 8. *a* — dependence of the transition temperature T_C to the superconducting state on the average particle size of molybdenum carbide *d*. The value for 0.1 μm was taken from [14] (marked in red); *b* — dependence of the critical field on the particle diameter *d*; *c* — temperature dependences of the critical field of the superconducting transition for molybdenum carbide powders with different magnitudes *d*. Solid line — approximation by the formula (1); *d* — coercive force H_F versus the particle diameter *d* at $T = 10$ K; *e* — coercive force H_F versus temperature for molybdenum carbide powders with different magnitudes *d*.

Conflict of interest

The authors declare that they have no conflict of interest.

References

[1] M.K. Kotel-Veetil, S.B. Qadri, M. Osofsky, T.M. Keller, R. Goswami, S.A. Wolf. J. Phys. Chem. C **111**, 16878-16882 (2007).
[2] P.W. Anderson. J. Phys. Chem. Solids **11**, 26 (1959).
[3] V.Z. Kresin, Y.N. Ovchinnikov. Phys. Rev. B **74**, 024514 (2006).
[4] H.M. Jaeger, D.B. Haviland, B.G. Orr, A.M. Goldman. Phys. Rev. B **40**, 182 (1989).
[5] B. Muhlschlegel, D.J. Scalapino, R. Denton. Phys. Rev. B **6**, 1767 (1972).
[6] D. Bono, A. Schnepf, J. Hartig, H. Schnockel, G.J. Nieuwenhuys, A. Amato, L. Jongh. Phys. Rev. Lett. **97**, 077601 (2006).
[7] J. Hartig, A. Schnepf, L.J. Jongh, D. Bono, H. Schnockel. Z. Anorg. Allg. Chem. **10**, 4504-4510 (2016).
[8] A. Gerber, A. Milner, G. Deutscher, M. Karpovsky, A. Gladkikh. Phys. Rev. Lett. **78**, 4277 (1997).
[9] L. Wang, C. Xu, Z. Liu, L. Chen, X. Ma, H.-M. Cheng, W. Ren, N. Kang. ACS Nano **10**, 4504-4510 (2016).
[10] D. Geng, X. Zhao, Z. Chen, W. Sun, W. Fu, J. Chen, W. Liu, W. Zhou, K.P. Loh. Adv. Mater. **29**, 1700072 (2017).
[11] X.Y. Lang, Q. Jiang. Solid State Comm. **134**, 797-801 (2005).
[12] M. Ido. J. Phys. Soc. Jpn. **41**, 412 (1976).
[13] C.Q. Sun, W.H. Zhong, S. Li, B.K. Tay, H.L. Bai, E.Y. Jiang. J. Phys. Chem. B **108**, 1080 (2004).
[14] B. Sun, L. Xu, K. Tang, L. Wang, Z. Ju, Y. Qian. Cryst. Res. Technol. **47**, 467-470 (2012).
[15] I.L. Landau, H.R. Ott. Phys. Rev. B **66**, 144506 (2002).
[16] H. Shu, W. Zhong, J. Feng, H. Zhao, Y. Chen, F. Hong, B. Yue. Acta Mater. **285**, 120693 (2025).
[17] D. Aoki, A. Huxley, E. Ressouche, D. Braithwaite, J. Flouquet, J.-P. Brison, E. Lhotel, C. Paulsen. Nature **413**, 613–616 (2001).
[18] C. Paulsen, D.J. Hykel, K. Hasselbach, D. Aoki. Phys. Rev. Lett. **109**, 237001 (2012).
[19] D. Aoki, J. Flouquet. J. Phys. Soc. Jpn **81**, 011003 (2012).
[20] M. Ishikawa, O. Fischer. Solid State Commun. **23**, 37–39 (1977).
[21] L.N. Bulaevskii, S.V. Panjukov. J. Low. Temp. Phys. **52**, 137–162 (1983).
[22] C. Pfleiderer, M. Uhlarz, S.M. Hayden, R. Vollmer, H. Lohneysen, N.R. Bernhoeft, G.G. Lonzarich. Nature **412**, 58–61 (2001).
[23] T. Shang, Y. Wang, B. Yu, K. Xia, D.J. Gawryluk, Y. Xu, Q. Zhan, J. Zhao, T. Shiroka. Phys. Rev. B **110**, 064510 (2024).

Translated by T.Zorina